



Electronic Delivery Cover Sheet

WARNING CONCERNING COPYRIGHT RESTRICTIONS

The copyright law of the United States (Title 17, United States Code) governs the making of photocopies or other reproductions of copyrighted materials. Under certain conditions specified in the law, libraries and archives are authorized to furnish a photocopy or other reproduction. One of these specified conditions is that the photocopy or reproduction is not to be "used for any purpose other than private study, scholarship, or research". If a user makes a request for, or later uses, a photocopy or reproduction for purposes in excess of "fair use", that user may be liable for copyright infringement. This institution reserves the right to refuse to accept a copying order if, in its judgement, fulfillment of the order would involve violation of copyright law.



Photoinduced electron transfer between dimethylaniline and oxazine 1 in micelles

Samir Kumar Pal, Debabrata Mandal, Dipankar Sukul, Kankan Bhattacharyya *

Physical Chemistry Department, Indian Association for the Cultivation of Science, Jadavpur, Calcutta 700 032, India

Received 17 May 1999

Abstract

Photoinduced electron transfer (PET) from *N,N*-dimethylaniline (DMA) to oxazine 1 (OX-1) is studied in micelles. It is observed that in anionic (sodium dodecyl sulfate, SDS) and neutral (Triton X-100, TX) micelles the rate of electron transfer (ET) from DMA to OX-1 is respectively 6.5 and 3 times smaller than that in water, and respectively 162 and 90 times smaller than that in neat DMA. The lower ET quenching constant in micellar media is ascribed to the greater donor–acceptor distance in the micelles. © 1999 Elsevier Science B.V. All rights reserved.

Keywords: Photoinduced electron transfer; Dimethylaniline; Oxazine 1

1. Introduction

Photoinduced electron transfer (PET) plays a crucial role in many chemical and biological processes [1–7]. The rate of electron transfer (ET) depends on various factors. This includes reorganization energy of the solvent and the reactants, electronic and vibronic coupling between the initial and the final states, solvent relaxation and vibrational relaxation. Recently, several groups reported ultrafast ET rates faster than the rate of solvation [8–15]. Barbara et al. [8,9] reported such ultrafast ET for intramolecular ET in betain dyes and in mixed valence complexes [10,11]. Yoshihara et al. [12–15], on the other hand,

reported ultrafast intermolecular ET in neat dimethylaniline (DMA) and other donors from the solvent to several acceptors e.g., oxazine 1 (OX-1), Nile blue, coumarins, etc. The ultrafast ET process is assisted by the solvation coordinate (X) as well as the intramolecular vibrational modes (q) [13–15]. When the ET process is faster than the solvent relaxation time, motion of the solvent molecules can be considered completely frozen during the ET process. In this case, the reactants (donor/acceptor) reach the transition state through motion along a vibrational coordinate, [1,2,8–18]. Bagchi et al. [16–18] have recently made a detailed theoretical analysis of this model delineating the role of different vibrational modes in the ultrafast ET process.

Though PET process in homogeneous solution has been studied quite thoroughly much less is known about the PET processes in organized media. In an

* Corresponding author. Fax: +91-33-473-2805; e-mail: pckb@mahendra.iacs.res.in

organized medium, the active chemical species is confined in a small volume. The local dielectric constant and viscosity of the microenvironments are often drastically different from those in a bulk liquid and also the effect of diffusion is minimized in the confined systems. Such confinement markedly retards the dynamics of many processes. Several groups have reported dramatic retardation of the solvation dynamics in cyclodextrin [19,20], reverse micelles/microemulsions [21–24], micelles [25], and other organized media. Similar retardation is also reported for intramolecular charge transfer processes [26,27] and isomerization dynamics [28] in these media.

Due to the importance of PET processes in biology and the fact that most biological processes occur in self-organized molecular assemblies, it is important to know how different organized assemblies affect the PET process. However, there have been relatively few studies on how the restricted motion of the donors and the acceptors in organized assemblies affect the PET process. Fayer et al. [29,30] studied photoinduced intermolecular ET from *N,N*-dimethylaniline (DMA) to hydrophobic rhodamine 6G (R6G) dyes in three cationic micelles, dodecyl-, tetradecyl- and cetyl trimethyl ammonium bromide (DTAB, TTAB and CTAB). Recent small angle X-ray and neutron scattering studies [31–34] have revealed detailed information on the structure of these micelles. These studies indicate that the core of any micelle is essentially dry and contain the alkyl chains. The “dry” core is surrounded by a spherical shell which contains the polar (for neutral Triton X-100, TX) or the ionic head groups (for cationic CTAB and anionic sodium dodecyl sulfate, SDS) and water molecules. The spherical shell is called Stern layer for an ionic micelle and palisade layer for a neutral one. NMR [35] and absorption spectra [29,30] of DMA in aqueous micellar solutions are significantly different from those in bulk water. This indicates that on binding to the micelles the DMA molecules experience an environment different from bulk water. The observed spectra suggest that the DMA molecules are located at the Stern layer of the micelles near the polar head groups where the polarity is less than of water but is higher than that of a hydrocarbon like environment. The cationic acceptor OX-1 also stays in the Stern layer due to its insolubility in the hydrocarbon core.

In the present work, we intend to find out how the ultrafast PET process between DMA and OX-1, which occurs in 0.2 ps timescale in neat DMA [12], is affected in micelles. Since OX-1 is a cationic dye it is expected to bind strongly with the anionic SDS and neutral TX micelles but not to the cationic CTAB micelles. Thus, one need not attach an alkyl chain to OX-1 to study PET from DMA to OX-1 in anionic and neutral micelles. The local concentration of the donor or quencher DMA molecules in the Stern layer of the micelles is obviously very high. Thus, at first sight one would expect a very high ET rate in the micelles. However, we will see that the ET rate is quite slow in micelles and we will discuss the possible reasons for the retardation of the ET process in micelles.

2. Experimental

OX-1 (Exciton), DMA (Aldrich) and the surfactants SDS, TX and CTAB (Aldrich) were used as received. The sample was excited at 600 nm using a synchronously pumped picosecond R6G dye laser (Coherent 702-1) pumped by a cw mode-locked Nd:YAG (Coherent, Antares). The emission was collected at magic angle polarization for lifetime measurement by a Hamamatsu MCP photomultiplier (2809-U). The typical system response at 600 nm excitation is about 100 ps. For rotational relaxation studies, emission intensity at perpendicular (I_{\perp}) and parallel (I_{\parallel}) polarizations were collected alternatively for 100 s. For a typical anisotropy decay a peak count of 10,000 counts were collected at parallel polarization. The $r(t)$ is then calculated using the relation

$$r(t) = \frac{I_{\parallel}(t) - GI_{\perp}(t)}{I_{\parallel}(t) + 2GI_{\perp}(t)}$$

The G factor of the setup was determined using a dye whose rotational relaxation time is very short (e.g., Nile red in methanol). For quantum yield measurement we used the laser dye 3,3'-diethyloxadicarbocyanine iodide (DODCI) in methanol ($\phi_f = 0.49$) [36] as standard. The rate constants for the radiative (k_r) and non-radiative (k_{nr}) decay are cal-

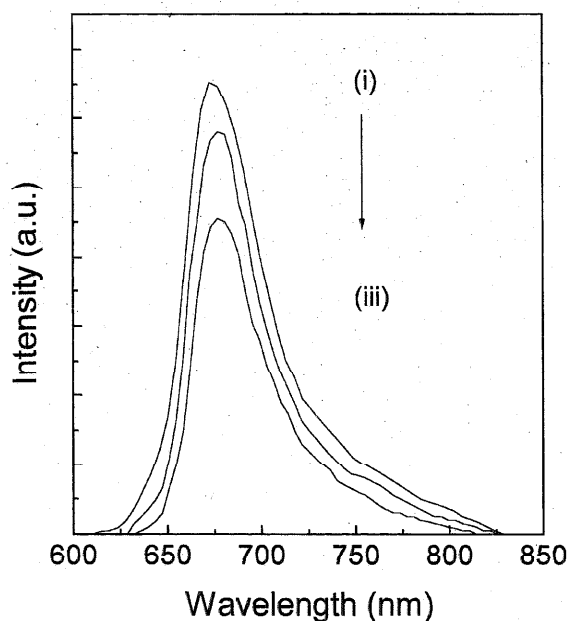


Fig. 1. Emission spectrum of 5×10^{-6} M OX-1 in water containing (i) 0 mM, (ii) 3.95 mM and (iii) 7.9 mM DMA.

culated using the relations $k_r = \varphi_f / \tau_f$ and $k_{nr} = (1 - \varphi_f) / \tau_f$.

3. Results

3.1. OX-1 in water

In aqueous solution, OX-1 exhibits a weak emission with quantum yield, $\varphi_f = 0.02$ and lifetime,

$\tau_f = 520 \pm 20$ ps. Its rotational relaxation time in water is 150 ± 25 ps. These values are consistent with the recent data of Balabai et al. [37]. DMA is sparingly soluble in neat water, (solubility $\approx 1 \mu\text{l}$ per ml of water). On addition of 7.9 mM DMA to an aqueous solution of OX-1, φ_f of OX-1 decreases to 0.014 and τ_f to 460 ± 20 ps. Fig. 1 describes the effect of DMA on emission intensity of OX-1 in water. The rate constant of ET between DMA and OX-1, k_{ET} can be defined as the difference in the non-radiative rate constant of OX-1 in water in the absence of DMA (k_{nr}^0) and that (k_{nr}) in the presence of DMA, so that $k_{ET} = k_{nr} - k_{nr}^0$. The k_{ET} is related to the quenching constant k_Q by the relation $k_{ET} = k_Q[Q]$, where $[Q]$ denote concentration of the quencher (DMA, in the present case). The quenching constant for quenching of OX-1 by DMA in aqueous medium is found to be $(2.5 \pm 0.5) \times 10^{10} \text{ s}^{-1} \text{ M}^{-1}$.

3.2. OX-1 in micelles

On addition of SDS and TX to an aqueous solution of OX-1, φ_f , τ_f and rotational relaxation time of OX-1 increase when the concentrations of the surfactants exceed their respective critical micellar concentration (CMC), i.e., when the micellar aggregates are formed. In the presence of CTAB micelles, however, the emission intensity, lifetime and rotational relaxation time of OX-1 remain same as those in water. This indicates that the cationic dye OX-1 does not

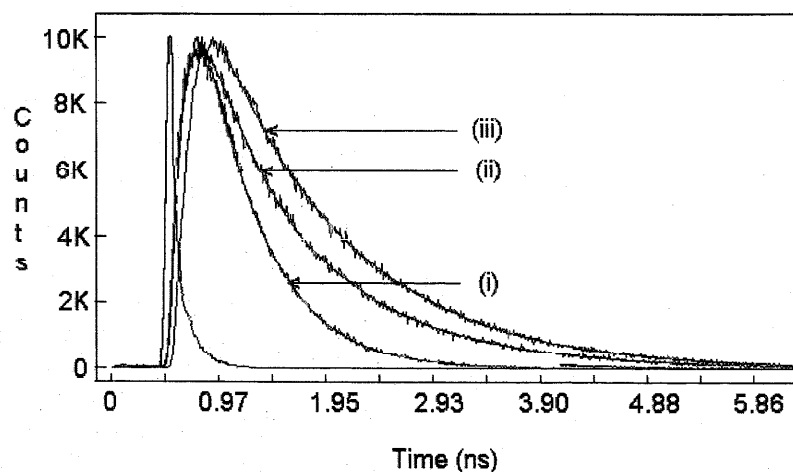


Fig. 2. Fluorescence decays of OX-1 at magic angle polarization in (i) water, (ii) 50 mM TX and (iii) 50 mM SDS.

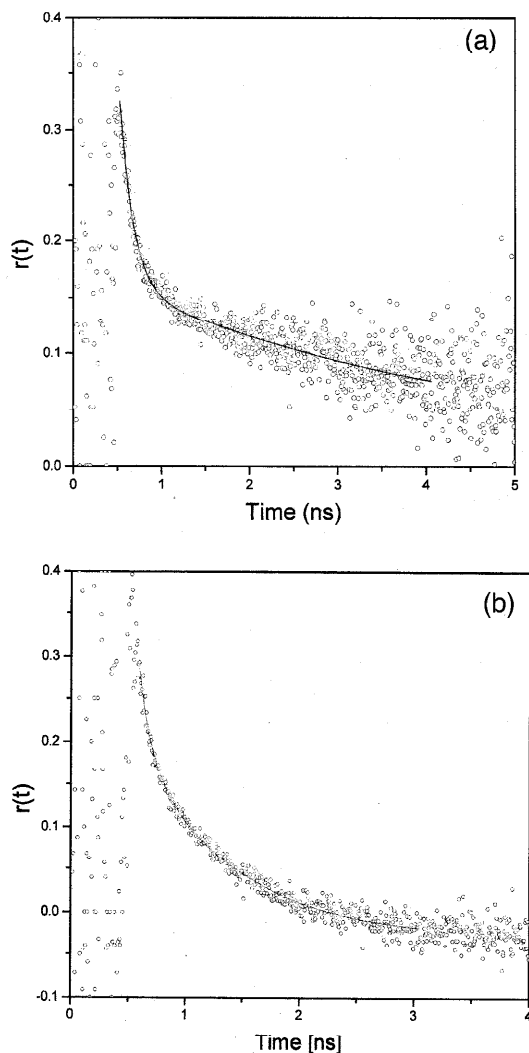


Fig. 3. Decays of fluorescence anisotropy of OX-1 in (a) 50 mM TX and (b) 50 mM SDS.

bind to the cationic micelle, CTAB. In 50 mM SDS, (CMC = 8 mM), ϕ_f of OX-1 increases to 0.047

while in 50 mM TX-100 (CMC = 0.26 mM) micelles, ϕ_f of OX-1 increases to 0.04. In the presence of the micelles the emission decays of OX-1 is observed to be multi-exponential. This is due to inherent inhomogeneity of the micellar media [38–40]. Instead of giving too much importance to individual decay components we have fitted the decays to a bi-exponential decay, $a_1 \exp(-t/\tau_1) + a_2 \exp(-t/\tau_2)$ and used the average lifetime $\langle \tau \rangle = a_1 \tau_1 + a_2 \tau_2$, to get an average picture (Table 2). In SDS micelles, the average lifetime of OX-1 increases to 1200 ± 20 ps and in 50 mM TX-100 it is 900 ± 20 ps. The fluorescence decay of OX-1 in water and in SDS and TX micelles are shown in Fig. 2. The increase in ϕ_f and τ_f indicate strong binding of OX-1 to SDS and TX-100 micelles.

The rotational relaxation times of OX-1 in these two micelles are also quite different from that in water. The rotational anisotropy decays of OX-1 in SDS and TX micelles are shown in Fig. 3. The rotational relaxation time (τ_R) of OX-1 in SDS and TX are biexponential with an average rotational relaxation time, $\langle \tau_{rot} \rangle (= a_{1r} \tau_{1r} + a_{2r} \tau_{2r})$ of 625 ± 25 ps for SDS and 2100 ± 100 ps for TX (Table 1). The rotational relaxation of OX-1 in micelles is considerably slower than in water (125 ± 25 ps). Balabai et al. [37] have reported that the rotational relaxation time of OX-1 increases to 400 ps when OX-1 binds to a β -cyclodextrin (β -CD) cavity. The rotational relaxation times of OX-1 in SDS and TX micelles are longer than that in β -CD [37]. This indicates that the motion of OX-1 is more restricted in micelles than in β -CD. This is not unreasonable as β -CD encloses only a part of the big dye molecule OX-1 and most of it is projected outward in bulk water. The emission lifetime of OX-1 in the presence of β -CD is marginally different from that in water [37], which implies that in the complex the OX-1 molecule remains very largely exposed to water.

Table 1
Emission properties of OX-1

Medium	ϕ_f	τ_f (ps)	a_{1r}	τ_{1r} (ps)	a_{2r}	τ_{2r} (ps)	$\langle \tau_{rot} \rangle^a$ (ps)
Water	0.02	520 ± 20	1.00	125 ± 25			150 ± 25
SDS	0.047	1200 ± 20	0.30	100	0.70	850	625 ± 25
TX-100	0.04	900 ± 20	0.50	150	0.50	4100	2100 ± 100

^aAverage rotational relaxation time $\langle \tau_{rot} \rangle = a_{1r} \tau_{1r} + a_{2r} \tau_{2r}$.

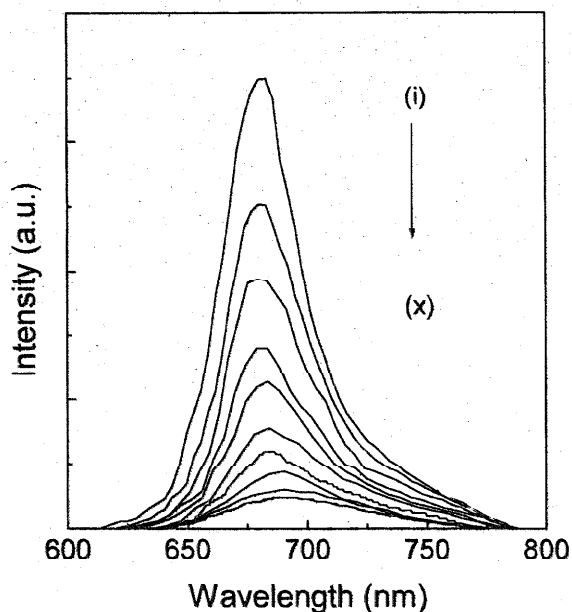


Fig. 4. Emission spectrum of OX-1 in 50 mM SDS containing (i–x) 0, 2.63, 5.27, 7.90, 10.54, 13.17, 15.81, 18.44, 21.00 and 23.71 mM DMA.

The biexponentiality of the rotational relaxation of various fluorescent probes in micelles have been reported by several groups [37,41,42]. The biexponentiality arises from the lateral diffusion of the probe in the Stern layer of the micelles and the coupling of the motion of the probe to that of the micelles. Various models such as the wobbling-in-a-

cone and the two step model have been used to explain the rotational relaxation in micelles [37,41,42]. We defer the analysis of the biexponential decay of OX-1 in micelles to a subsequent publication. For the purpose of PET in micelles it will suffice to conclude that the rotational motion of OX-1 in micelles is significantly slower than that in water. The slow rotational dynamics is not due to the electrostatic attraction between the cationic dye and the anionic micelles (SDS), as the rotational relaxation is slower in the neutral micelle TX than in anionic SDS. It appears that in the micelles, the probe gets entangled within the surfactant molecules and this reduces its mobility.

3.3. PET from DMA to OX-1 in micelles

In the presence of SDS micelles, solubility of DMA in water increases nearly three times. On gradual addition of DMA to an aqueous solution of OX-1 containing 50 mM SDS, ϕ_f and $\langle\tau\rangle$ of OX-1 decreases markedly (Figs. 4 and 5; Tables 2 and 3). At the maximum concentration of DMA, τ_f of OX-1 decreases to 210 ps. The ET rate is calculated once again using the relation, $k_{ET} = k_{nr} - k_{nr}^0$, where k_{nr}^0 is the rate constant of non-radiative decay of OX-1 in SDS micelles in the absence of DMA and k_{nr} is that in the presence of DMA. In the case of SDS, the magnitude of k_{ET} at the maximum [DMA], is $(4.0 \pm 0.1) \times 10^9 \text{ s}^{-1}$, which is nearly 16 times faster than that at the maximum DMA concentration in water.

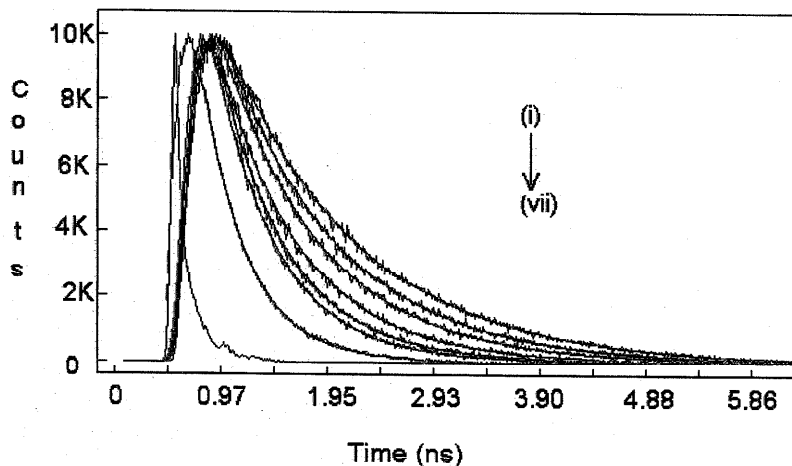


Fig. 5. Fluorescence decays of OX-1 in 50 mM SDS containing (i–vii) 0, 2.63, 5.27, 7.90, 10.54, 13.17 and 23.71 mM DMA.

Table 2
Rate of PET from DMA to OX-1 in different media

Medium	DMA (mM)	a_1	τ_1 (ps) ^a	a_2	τ_2 (ps) ^a	$\langle\tau\rangle$ (ps)
50 mM SDS	0.00	1	1200			1200
	5.27	0.37	260	0.63	900	660
	7.90	0.45	200	0.55	740	500
	10.54	0.47	200	0.53	620	420
	13.17	0.49	200	0.51	560	380
	15.81	0.52	185	0.48	510	340
	18.44	0.48	160	0.52	440	310
	21.08	0.59	130	0.41	390	230
	23.71	0.61	130	0.39	340	210
50 mM TX-100	0.00	0.40	460	0.60	1170	890
	2.63	0.44	480	0.56	1050	800
	5.27	0.49	440	0.51	950	700
	10.54	0.45	340	0.55	810	600
	15.81	0.35	260	0.65	680	530
	21.08	0.36	260	0.64	630	500

^a ± 20 ps.

It is evident that the emission lifetime, quantum yield and the rotational relaxation time of OX-1 in the presence of micelles are substantially different from those in water. This indicates that in the presence of the micelles the dye molecules migrate from bulk water to the micellar aggregates. Since the charged OX-1 molecule is insoluble in the hydrocar-

bon core of the micelles it is apparent that OX-1 molecules reside in the polar Stern layer of the micelles. The absorption [29,30] and NMR spectra of DMA in micellar media are very different from those in bulk water and according to several groups this indicates that the donor DMA molecules reside in the Stern layer of the micelles [29,30,35]. Since the Stern layer is a thin spherical shell of thickness about 9 Å for SDS and 25 Å for TX, the donor (DMA) and the acceptor (OX-1) stay in close proximity in the Stern layer.

For the determination of the quenching constant, k_Q , in the micellar environment, it is necessary to find out the concentration of DMA molecules in the Stern layer of the micelles. According to the SANS study, the overall radius of the SDS micelles is 30 Å and the Stern layer is about 9 Å thick [31–34]. Thus, the volume of the spherical shell of the Stern layer is $(4\pi/3) [30^3 - 21^3] \text{ \AA}^3$. The number of DMA molecules per micelle can be calculated by dividing the total DMA concentration by the micellar concentration ($[M]$). The latter, $[M]$ is given by $[M] = \{[S] - \text{CMC}\} / N_{\text{ag}}$, where $[S]$ is the total surfactant (SDS) concentration, CMC is the critical micellar concentration (8 mM for SDS) and N_{ag} is the aggregation number (74 for SDS). The local concentration

Table 3
Rate of PET from DMA to OX-1 in different media

Medium	[DMA] (mM)	[DMA] ₁ ^a (M)	ϕ_f^b	$\langle\tau\rangle$ (ps) ^c	$k_r \times 10^{-9}$ (s ⁻¹)	$k_{nr} \times 10^{-9}$ (s ⁻¹)	$k_{ET} \times 10^{-9}$ (s ⁻¹)	$k_Q \times 10^{-9}$ (s ⁻¹ M ⁻¹)
50 mM SDS	0.00	0.00	0.047	1200	0.04	0.79		
	5.27	0.21	0.026	660	0.04	1.47	0.68	3.25
	7.90	0.31	0.021	500	0.04	1.96	1.17	3.80
	10.54	0.41	0.016	420	0.04	2.34	1.55	3.80
	13.17	0.52	0.011	380	0.03	2.60	1.81	3.50
	15.81	0.62	0.008	340	0.03	2.91	2.12	3.40
	18.44	0.73	0.006	310	0.03	3.20	2.41	3.40
	21.08	0.83	0.004	230	0.02	4.33	3.54	4.30
	23.71	0.94	0.003	210	0.02	4.74	4.00	4.20
50 mM TX-100	0.00	0.00	0.039	890	0.04	1.08		
	2.63	0.019	0.032	800	0.04	1.21	0.13	6.80
	5.27	0.038	0.025	700	0.04	1.39	0.31	8.20
	10.54	0.076	0.019	600	0.04	1.63	0.55	7.20
	15.81	0.115	0.018	530	0.04	1.85	0.77	6.70
	21.08	0.152	0.013	500	0.03	1.97	0.90	5.90

^a[DMA]₁ denotes concentration of DMA in the Stern layer of the micelles.

^b $\pm 5\%$.

^c ± 20 ps.

$[\text{DMA}]_i$ of DMA in the Stern layer of the micelle is obtained by dividing the number of DMA molecules per micelle by the volume of the Stern layer. The local concentration ($[\text{DMA}]_i$) so obtained and the quenching constant, $k_Q (= k_{\text{ET}}/[\text{DMA}]_i)$ is listed in Table 3. It is readily seen that in the micelles, the k_Q is more or less independent of the DMA concentration and is equal to $(3.8 \pm 0.5) \times 10^9 \text{ s}^{-1} \text{ M}^{-1}$. This is nearly 6.5 times smaller than the quenching constant in water.

For neutral TX micelles, similar decrease in ϕ_f and τ_f of OX-1 is observed on addition of DMA to an aqueous solution of OX-1 containing 50 mM TX. The solubility of DMA in TX micelles is found to be slightly less than that in the case of SDS micelles. The value of k_{ET} at maximum $[\text{DMA}]_i$ in TX is found to be $(0.9 \pm 0.1) \times 10^9 \text{ s}^{-1}$, i.e., 3.5 times that at maximum $[\text{DMA}]$ in water. The quenching constant is obtained by calculating $[\text{DMA}]_i$, as discussed in the case of SDS, using the structural parameter of TX (overall radius 50 Å, thickness of the palisade layer 25 Å and aggregation number 100) [31–34]. The result summarized in Table 3 indicates that the quenching constant is $(7 \pm 1.2) \times 10^9 \text{ s}^{-1} \text{ M}^{-1}$, i.e., about three times smaller than that in water.

4. Discussion

According to Rubtsov et al. [12], while the fastest component of ET from DMA to OX-1 in neat DMA is 60 fs (80%), there are three other components of 200 fs (19%), 3 ps (1%) and 40 ps (0.3%) so that the average time constant of ET is 0.2 ps and the rate constant is $5 \times 10^{12} \text{ s}^{-1}$. Considering the concentration of neat DMA is 7.9 M, the quenching constant in neat DMA is $6.3 \times 10^{11} \text{ s}^{-1} \text{ M}^{-1}$. This value is about 25 times higher than that in water and respectively, 90 and 162 times higher than that in TX and SDS micelles. The time constant of 0.2 ps is close to the vibrational periods of a standard organic molecule. Thus, the ultrafast ET observed in neat DMA has been attributed to the vibrational modes of the reactants [12–18]. In the case of the micelles, the 90 or 162 times slower quenching constant is too slow to be attributed to any vibrational mode. Thus, the slow ET rate in micelles does not appear to be due to the vibrational motions of the donor or accep-

tor. The effect of solvent relaxation also appears to be minor as the probe oxazine molecule exhibits very slight change in dipole moment on electronic excitation and is a weak solvation probe [12]. Femtosecond studies show that in neat liquids OX-1 exhibits little or no wavelength dependence of emission decays [12]. This suggests that the role of solvation dynamics is minor in the case of PET from DMA to OX-1.

In water, the ET is essentially controlled by the diffusion of the donor and the acceptors. However, in neat DMA, the acceptor (OX-1) is always in contact with the donor and role of diffusion is unimportant. In the case of the micelles the diffusion of the reactants is highly restricted as both the donor and the acceptor are constrained to remain in the thin Stern layer. The presence of the surfactant molecules in between the acceptor (OX-1) and the donor (DMA) molecule results in an increase in the donor–acceptor distance in the micelles compared to that in neat DMA. Tavernier et al. [29,30] recently presented a very rigorous analysis of the distance dependent ET rate in micelles taking into account diffusion. However, we will use the simpler approach discussed by Rubtsov et al. [12] to show that the increase in the donor–acceptor distance causes significant decrease in the rate constant of ET between in DMA and OX-1 in micelles.

According to the Marcus theory, the rate constant of ET decreases markedly with increase in the donor–acceptor distance (R). In the micelles, due to incorporation of the donor and the acceptor among the surfactant molecules the donor–acceptor distance increases significantly compared to that in neat DMA. The electronic coupling strength between the donor and the acceptor decreases exponentially with R as $\exp(-\beta R)$ where $\beta = 1 \text{ \AA}^{-1}$ [1,2,12,29,30]. This term decreases 2.72 and 4.5 times for an increase of R by 1 and 1.5 Å, respectively. The distance, R also affects the reorganization energy of the solvents (λ_s). λ_s is given by

$$\lambda_s = (e^2/2)(r_D^{-1} + r_A^{-1} - 2R^{-1})(n^{-2} - \epsilon^{-1})$$

where r_D , r_A are respectively the radii of the donor (2.5 Å for DMA) and the acceptor (4.2 Å for OX-1) molecules, n and ϵ are respectively the refractive index and the dielectric constant of the medium. The overall reorganization energy, $\lambda = \lambda_s + \lambda_i$, where

the internal reorganization energy (λ_i) for DMA and OX-1 is 0.5 eV [12]. The overall ET rate constant is related to λ as $\exp[-(\Delta G^0 + \lambda)^2/4\lambda RT]$. For DMA/OX-1 system, $\Delta G^0 = -0.68$ eV [12]. As a result the factor $\exp[-(\Delta G^0 + \lambda)^2/4\lambda RT]$, decreases by 1.15 and 1.45 times for an increase in R by 1 and 1.5 Å, respectively, from the value 3.8 Å in neat DMA [12]. Combining the effect of change in the coupling strength and the reorganization energy the ET rate constant decreases by 3.15 and 6.5 times for an increase in R by 1 and 1.5 Å, respectively. Thus, the change in quenching constant in going from water to micelles could be due to an increase in the donor–acceptor distance (R) by 1–1.5 Å in the micellar media.

The micellar interface resembles an alcohol ($n \approx 1.36$ and $\epsilon \approx 30$). As a result, the factor $(n^{-2} - \epsilon^{-1})$ changes from 0.55 in water to 0.51 in micelles. This causes the ET rate to increase by a factor of 1.3 in micelles compared to water. Thus, the observed smaller ET rate in micelles is not due to the lower dielectric constant of the micellar microenvironment.

5. Conclusions

The present study indicates that the cationic dye, OX-1 binds quite strongly with the anionic SDS and neutral TX micelles as indicated by the increase in emission intensity, lifetime and rotational relaxation time. The cationic dye however, does not bind with the cationic micelles, CTAB. It is observed that in the presence of the micelles, the solubility of DMA increases in water and the PET rate increases respectively 16 and 3.5 times in SDS and TX micelles, compared to that in aqueous medium. However, due to the very high local concentration of the DMA at the micellar surface the quenching constant of OX-1 for DMA in micelles are respectively 6.5 and 3 times smaller in SDS and TX micelles than that in water. The role of vibrational relaxation and solvation appears to be minor to explain the lower rate of ET in micelles. The lower quenching constant due to PET in micellar media is attributed to an increase in the donor–acceptor distance, R , by 1–1.5 Å in the micellar media.

Acknowledgements

Thanks are due to Department of Science and Technology (DST) and Council of Scientific and Industrial Research (CSIR), Government of India, for generous research grants. CSIR is also thanked for providing fellowship to SKP, DM and DS.

References

- [1] R.A. Marcus, *Rev. Mod. Phys.* 65 (1993) 599, and references therein.
- [2] H. Sumi, R.A. Marcus, *J. Chem. Phys.* 84 (1986) 4272.
- [3] M. Heitele, *Angew. Chem., Int. Ed. Engl.* 32 (1993) 359.
- [4] J.R. Miller, L.T. Calcaterra, G.L. Closs, *J. Am. Chem. Soc.* 106 (1984) 3047.
- [5] M. Bixon, J. Jortner, *Chem. Phys.* 176 (1993) 467.
- [6] D.F. Calef, P.G. Wolynes, *J. Phys. Chem.* 87 (1983) 3387.
- [7] I. Rips, J. Jortner, *J. Chem. Phys.* 87 (1987) 2090.
- [8] G.C. Walker, E. Akesson, A.E. Johnson, N.E. Levinger, P.F. Barbara, *J. Phys. Chem.* 96 (1992) 3728.
- [9] P.J. Reid, C. Silva, P.F. Barbara, *J. Phys. Chem.* 99 (1995) 3554.
- [10] D.A.V. Kliner, K. Tominaga, G.C. Walker, P.F. Barbara, *J. Am. Chem. Soc.* 114 (1992) 8323.
- [11] K. Tominaga, D.A.V. Kliner, A.E. Johnson, N.E. Levinger, P.F. Barbara, *J. Chem. Phys.* 98 (1993) 1228.
- [12] I.V. Rubtsov, H. Shirota, K. Yoshihara, *J. Phys. Chem. A* 103 (1999) 1801.
- [13] Y. Nagasawa, A.P. Yartsev, K. Tominaga, A.E. Johnson, K. Yoshihara, *J. Chem. Phys.* 101 (1994) 5717.
- [14] H. Shirota, H. Pal, K. Tominaga, K. Yoshihara, *Chem. Phys.* 236 (1998) 355.
- [15] H. Pal, Y. Nagasawa, K. Tominaga, K. Yoshihara, *J. Phys. Chem.* 100 (1996) 11964.
- [16] N. Gayathri, B. Bagchi, *J. Phys. Chem.* 100 (1996) 9207.
- [17] S. Roy, B. Bagchi, *J. Phys. Chem.* 98 (1994) 3056.
- [18] B. Bagchi, N. Gayathri, *Adv. Chem. Phys.* 89 (1998) 1.
- [19] N. Nandi, B. Bagchi, *J. Phys. Chem.* 100 (1996) 13914.
- [20] S. Vajda, R. Jimenez, S. Rosenthal, V. Fidler, G.R. Fleming, E.W. Castner Jr., *J. Chem. Soc., Faraday Trans.* 91 (1995) 867.
- [21] J.S. Lundgren, M.P. Heitz, F.V. Bright, *Anal. Chem.* 67 (1995) 3775.
- [22] S. Das, A. Datta, K. Bhattacharyya, *J. Phys. Chem. A* 101 (1997) 3299.
- [23] R.E. Riter, D.M. Willard, N.E. Levinger, *J. Phys. Chem. B* 102 (1998) 2705.
- [24] H. Shirota, K. Horie, *J. Phys. Chem. B* 103 (1999) 1437.
- [25] N. Sarkar, A. Datta, S. Das, K. Bhattacharyya, *J. Phys. Chem.* 100 (1996) 15483.
- [26] C.B. Cho, M. Chung, J. Lee, T. Nguyen, S. Singh, M.

- Vedamuthu -B., S. Yao, S.-B. Zhu, Robinson, J. Phys. Chem. 99 (1995) 7806.
- [27] A. Datta, D. Mandal, S.K. Pal, K. Bhattacharyya, J. Phys. Chem. B 101 (1997) 10221.
- [28] S.K. Pal, A. Datta, D. Mandal, K. Bhattacharyya, Chem. Phys. Lett. 288 (1998) 793.
- [29] H.L. Tavernier, A.V. Barzykin, M. Tachiya, M.D. Fayer, J. Phys. Chem. B 102 (1998) 6078.
- [30] K. Weidemaier, H.L. Tavernier, S.F. Swallen, M.D. Fayer, J. Phys. Chem. A 101 (1997) 1887.
- [31] H.H. Pardies, J. Phys. Chem. 84 (1980) 599.
- [32] S.S. Berr, J. Phys. Chem. 91 (1987) 4760.
- [33] S.S. Berr, M.J. Coleman, R.R.M. Jones, J.S. Johnson, J. Phys. Chem. 90 (1986) 6492.
- [34] S.S. Berr, E. Caponetti, R.R.M. Jones, J.S. Johnson, L.J. Magid, J. Phys. Chem. 91 (1987) 5766.
- [35] J.C. Eriksson, G. Gilberg, Acta Chim. Scand. 20 (1966) 2019.
- [36] S.P. Velsko, G.R. Fleming, Chem. Phys. 65 (1982) 59.
- [37] N. Balabai, B. Linton, A. Nappaer, S. Priyadarshy, A.P. Sukharevsky, D.H. Waldeck, J. Phys. Chem. B 102 (1998) 9617.
- [38] C.H. Cho, M. Chung, J. Lee, T. Nguyen, S. Singh, M. Vedamuthu, S. Yao, S.-B. Zhu, G.W. Robinson, J. Phys. Chem. 99 (1995) 7806.
- [39] D. Topygin, J. Svodva, I. Konopasek, L. Brand, J. Chem. Phys. 96 (1992) 7919.
- [40] D.R. James, W.R. Ware, Chem. Phys. Lett. 120 (1985) 485.
- [41] E.L. Quitevis, A.H. Marcus, M.D. Fayer, J. Phys. Chem. 97 (1993) 5762.
- [42] M.M.G. Krishna, N. Periasamy, Chem. Phys. Lett. 298 (1998) 359.